Springer

KSME

Journal of Mechanical Science and Technology 27 (8) (2013) 2413~2423
www.springerlink.com/content/1738-494x
DOI 10.1007/s12206-013-0627-4

Internal stress analysis of a stepped rounded D-ring under a uniform squeeze rate and internal pressure using a photoelastic experimental hybrid method †

Bruno Robert Mose[1], Jeong Hwan Nam[2], Lim Hyun Seok[1] and Jai-Sug Hawong[1,*]

[1]*School of Mechanical Engineering, Yeungnam University, 214-1, Dae-dong, Gyeongsan, Gyeongbuk 712-749, Korea*
[2]*Department of Railroad Vehicle Engineering, Dongyang University, 145 Dongyangdaero, Punggi Yeongju, Gyeongbuk, 750-711, Korea*

(Manuscript Received February 17, 2013; Revised May 11, 2013; Accepted May 29, 2013)

Abstract

Internal stresses occurring in a stepped rounded D-ring compressed to 20% squeeze and pressurized with internal pressures of 0, 0.98, 1.96, 2.94, 3.92 and 4.9 MPa are analyzed using a photoelastic experimental hybrid method. At a pressure of 0 MPa and 20% squeeze, the photoelastic isochromatic fringes of the stepped rounded D-ring were almost symmetrical. As the internal pressure increased, the isochromatics shifted and curved towards the extrusion gap. By supplying a radius of 0.33 mm at the corners of the stepped D-ring, the high stresses at the sharp corners were reduced by up to 25%. These results further indicate that extrusion of the stepped rounded D-ring occurred at an internal pressure of 4.9 MPa which was about 25% higher than the pressure at which the extrusion of the stepped unrounded D-ring occurred.

Keywords: D-ring; Squeeze rate; Internal pressures; Extrusion; Contact stresses; Photoelastic experimental hybrid method

1. Introduction

Seals are critical components in mechanical systems and are used to prevent lubricants from leaking into sealed compartments [1, 2]. O-ring seals are widely used. However, the cross sectional area of an O-ring becomes less than optimal for sealing applications because a significant portion of the seal is often sheared during installation [3]. Moreover, the circular cross section of the O-ring makes it susceptible to spiral failure, and this can strongly affect its performance, especially in dynamic applications [4]. In recent years, encouraging progress has been made in developing seals with different cross sectional configurations designed to improve their sealing ability.

The D-ring has been suggested as an alternative to the common O-ring. The flat base of the D-ring has been reported to contribute significantly to its stability in addition to reducing chances of spiral failure or twisting as is commonly cited [5].

In many applications, high stresses develop in seals [6]. Therefore, it is important that a detailed analysis of the stresses in seals be conducted in order to minimize leakages and enhance the performance of the mechanical systems that use the seals. There are currently three methods for determining the stresses arising from contact problems. : theoretical (or analytical), computational, and experimental.

Among the experimental stress analysis methods, photoelasticity has received considerable attention as a tool for investigating assembly stresses such as those in O-rings and other sealing elements because of the advantages it offers compared to other methods. Several investigators have used photoelasticity to study the stresses arising from seals. Strozzi [7] analyzed the static stresses of an unpressurized, rounded, rectangular elastomeric seal using photoelasticity and showed remarkable agreement between experimental and theoretical values. Medri and Strozzi [8] performed photoelatic studies using polyurethane models and noted good agreement between the experimental and the numerical isochromatic fringe patterns. Bignardi el al. [9] conducted photoelastic measurements using both isoclinic and isochromatic data to describe the stress fields and contact pressures of a lip seal.

In this study, we perform a detailed analysis of the stresses in a stepped and rounded D-ring under uniform squeeze and internal pressure. An understanding of the stresses occurring in a D-ring under the described loading conditions will be useful in the design of D-rings and in enhancing their use in applications without twisting. The goals of this study are as follows; (i) determination of the optimal fillet radius of a stepped D-ring with $H_1/H_2 = 1$ using the finite element method(FEM), (ii) experimental analysis of the internal stress components, principal stresses and von Mises stresses of a

*Corresponding author. Tel.: +82 53 810 2445, Fax.: +82 53 810 4627
E-mail address: jshawong@ynu.ac.kr
† Recommended by Associate Editor Seong Beom Lee

stepped rounded D-ring with an optimal fillet radius under a uniform squeeze rate and internal pressure, (iii) determination of the relationship between the internal stress components, principal stresses, von Mises stresses, and internal pressures of a stepped rounded D-ring under a uniform squeeze rate and internal pressure, (iv) determination of the extrusion pressure of a stepped rounded D-ring under uniform squeeze rate and internal pressure, and (v) comparison between the internal stress components of a stepped un-rounded and stepped rounded D-ring under a uniform squeeze rate and internal pressure.

2. Basic theory

2.1 Hertz contact theory

Eq. (1) shows the stress components of a plane problem using Muskhelishvilli's potential functions Φ and ψ [10]. As shown in Eq. (1), the stress components are composed of two complex functions, Φ(z) and ψ(z). If the two complex functions are known, the stress components can be determined.

$$\begin{aligned}\sigma_X &= \mathrm{Re}\left[2\Phi(z)-\bar{z}\Phi'(z)-\Psi(z)\right]\\ \sigma_Y &= \mathrm{Re}\left[2\Phi(z)+\bar{z}\Phi'(z)+\Psi(z)\right]\\ \tau_{XY} &= \mathrm{Im}\left[\bar{z}\Phi'(z)+\Psi(z)\right].\end{aligned} \tag{1}$$

Contact problems are generally half-plane problems. If the upper portion of a body (z > 0) is a half-plane, the complex functions Φ and ψ are involved in the region. Therefore, in the half-plane of the lower portion of the body (z < 0), an analytic complex function is defined by Eq. (2a) [11]. The relative equation, Eq. (2b) between Φ(z) and ψ(z) is obtained from Eq. (2a). Thus,

$$\phi(\bar{z}) = -\overline{\Phi(z)} - \bar{z}\overline{\Phi'(z)} - \overline{\Psi(z)} \tag{2a}$$

$$\Psi(z) = -\Phi(z) - \overline{\Phi(\bar{z})} - z\Phi'(z). \tag{2b}$$

Since stress functions Φ(z) and ψ(z) are analytic functions, they can be represented in a power series form, as shown in Eq. (3).

$$\Phi(z) = \sum_{n=0}^{N} C_n z^{\frac{n}{2}} \tag{3a}$$

$$\Psi(z) = \sum_{n=0}^{N} D_n z^{\frac{n}{2}}. \tag{3b}$$

Substituting Eq. (3) into Eq. (2b), the relative equation between the complex coefficients of the complex function is determined, as shown in Eq. (4):

$$D_n = -\frac{n}{2}C_n - \bar{C}_n. \tag{4}$$

Eq. (5) is determined by substituting the relative equation between the complex coefficients of the complex function into the stress functions and substituting the resulting stress functions into Eq. (1),:

$$\begin{aligned}\sigma_X(Z) &= \sum_{n=1}^{N}\mathrm{Re}\left\{C_n\left[2F(n,z)-G(n,z)\right]+\bar{C}_nF(n,z)\right\}\\ \sigma_Y(Z) &= \sum_{n=1}^{N}\mathrm{Re}\left\{C_n\left[2F(n,z)+G(n,z)\right]-\bar{C}_nF(n,z)\right\}\\ \tau_{XY}(Z) &= \sum_{n=1}^{N}\mathrm{Im}\left\{C_nG(n,z)-\bar{C}_nF(n,z)\right\}\end{aligned} \tag{5}$$

where $F(n,z)=\frac{n}{2}z^{\frac{n}{2}-1}$, and

$G(n,z)=\frac{n}{2}\left[\left(\frac{n}{2}-1\right)\bar{z}-\frac{n}{2}z\right]z^{\frac{n}{2}-2}$.

2.2 Photoelastic experimental hybrid method

Eq. (6a) describes the stress optic law for an isotropic material [12]:

$$\left(\frac{f_\sigma\cdot N_f}{t}\right)^2 = (\sigma_X-\sigma_Y)^2+(2\tau_{XY})^2 \tag{6a}$$

$$\left(\frac{f_\sigma\cdot N_f}{t}\right)^2 - (\sigma_X-\sigma_Y)^2-(2\tau_{XY})^2 = D(\varepsilon) \tag{6b}$$

where f_σ is the stress fringe value, N_f is the fringe order, and t is the thickness of the specimen. After substituting the precise experimental data into Eq. (6a), errors are produced as shown in Eq. (6b). Therefore, D(ε) cannot be zero. In order to minimize the errors, the Hook-Jeeves numerical method [13] was used with the limiting condition of $D(\varepsilon)\le 10^{-5}$. By substituting Eq. (5) in Eq. (6b), Eq. (7) is obtained as follows:

$$\begin{aligned}D(\varepsilon) = &\left(\frac{f_\sigma\cdot N_f}{t}\right)^2\\ &-\left\{\sum_{n=1}^{N}a_n\,\mathrm{Re}\left[2F(n,z)-2G(n,z)\right]\right.\\ &\left.+\sum_{n=1}^{N}b_n\,\mathrm{Im}\left[2F(n,z)+2G(n,z)\right]\right\}^2\\ &-\left\{\sum_{n=1}^{N}a_n\,\mathrm{Im}\left[2G(n,z)-2F(n,z)\right]\right.\\ &\left.+\sum_{n=1}^{N}b_n\,\mathrm{Re}\left[2F(n,z)+2G(n,z)\right]\right\}^2.\end{aligned} \tag{7}$$

When the measured fringe orders (N_f), the position coordinates of the measured fringe orders (z = x + iy), the thickness of the specimen (t), and the stress fringe value (f_σ) are substituted into Eq. (7), the equation becomes a function of a_n and b_n

(a) Metallic D-ring

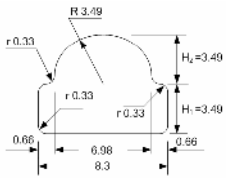

(b) Cross section of D-ring

Fig. 1. D-ring.

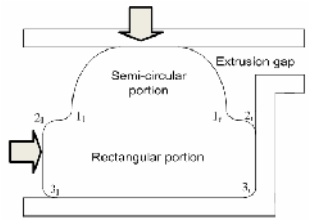

(a) D-ring loading condition

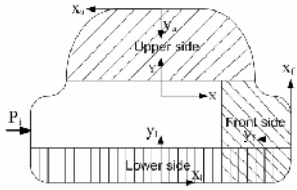

(b) Co-ordinate system

Fig. 2. Loading condition and co-ordinate system of D-ring. (Horizontal arrow is the direction of application of internal pressure. Vertical arrow is the direction of compression. (X,Y) is the global co-ordinate system. (xi,yi) is the local co-ordinate system.)

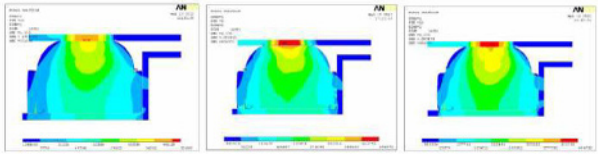

(a) 0.1 mm (b) 0.2 mm (c) 0.3 mm

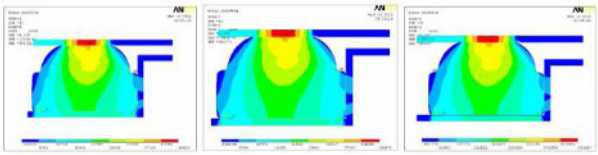

(d) 0.33 mm (e) 0.35 mm (f) 0.4 mm

Fig. 3. Variation of stress field as the fillet radius increased from 0.1 to 0.4 mm.

only. Applying the Hook-Jeeves numerical method to Eq. (7) with the experimental data, a_n and b_n are determined when the limit of errors is satisfied. Putting the values of a_n and b_n into the corresponding equation, the stress functions $\Phi(z)$ and $\psi(z)$ are obtained. Substituting the determined $\Phi(z)$ and $\psi(z)$ into Eq. (1), the stress components σ_X, σ_Y , and τ_{XY} produced in a structure under an arbitrary load can be determined. The principal stresses, σ_1, σ_2, and τ_{12} were obtained using the determined stress components σ_X, σ_Y, and τ_{XY} and the von Mises stresses σ_{VM} were obtained from the principal stresses [14]. These procedures comprise the proposed photoelastic experimental hybrid method [15].

3. Experimental method

First, a finite element analysis was carried out on a stepped D-ring model with a ratio of H_1/H_2 = 1 under a uniform squeeze of 20% to determine the optimal fillet radius. With an optimal fillet radius of 0.33 mm, a stepped D-ring hereafter referred to as the stepped rounded D-ring and the first of its kind was fabricated from aluminum metal having a plan diameter of 121.5±0.94 mm and a cross sectional height H of 6.98±0.15 mm as shown in Fig. 1.

A D-ring with a ratio of H_1/H_2 = 1 has been widely used in industrial fields.

The metallic D-ring model was placed in a molding box made from glass plates. Wet pink silicone prepared from a mixture of KE-1402 and CAT-1402 at a ratio of 10:1 by weight was poured into the molding box and allowed to harden for 12 hours. The metallic D-ring was removed from the mold to form a mold cavity whose shape is identical to the actual D-ring.

Photoelastic models of the stepped rounded D-ring were cast using Araldite B41 and hardener HT 903 (Ciba-Geigy Company, Japan) at a weight ratio (Araldite-to-hardener) of 10:3 according to the procedure described by Hawong, Han and Nam [15].

Stress freezing of the stepped rounded D-rings loaded at various internal pressures and compressed to a 20% squeeze rate (Fig. 2(a)) was carried out using the method described in Ref. [15].

Two-millimeter slices were cut from the stress frozen stepped rounded D-rings at intervals of 90˚ and polished using silicon carbide paper until their thickness was about 1 mm. The finished slices were put in a glass box containing a solution of α-bromonaphthalene and paraffin at a volume ratio of 1:0.585. A solution of α-bromonaphthalene and paraffin has almost the same refractive index as epoxy resin making it possible to obtain images of high clarity with reduced the scattering of light at the surfaces. The glass box with the finished slices was placed on the loading position of the transparent photoelastic experimental device and isochromatic fringe patterns were recorded using a digital camera.

The isochromatic fringe patterns obtained from the experiment were used to regenerate graphic isochromatics using a computer-based program. The regenerated fringes were compared with the actual photoelastic fringes. If the regenerated fringes were not similar to the actual ones, corrective steps were taken and the analysis was repeated until the two fringe patterns showed a good fit. Since it was not possible to apply the hybrid method to the whole area of the D-ring, the analysis was carried out independently for the upper and front sides of the D-ring using the coordinate system described in Fig. 2(b).

4. Results and discussion

In Fig. 3, results from a finite element analysis of a stepped rounded D-ring with a ratio of H_1/H_2 = 1 modeled under a uniform squeeze of 20% are shown indicating the maximum stresses due to fillet radii of 0.1, 0.2, 0.3, 0.33, 0.35, and 0.4

Table 1. Variation of maximum stress with fillet radius.

Fillet radius (mm)	0.1	0.2	0.3	0.33	0.35	0.4
Maximum stress (MPa)	0.446	0.386	0.323	0.269	0.269	0.269

Note: On the boundary, $\sigma_{VM}=\sigma_{max,}$ σ_{VM} = Von Mises equivalent stress

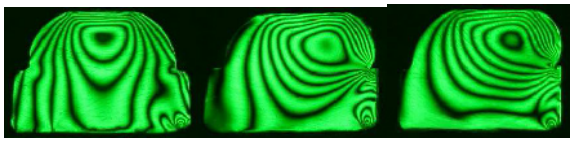

(a) 0 MPa (b) 0.98 MPa (c) 1.96 MPa

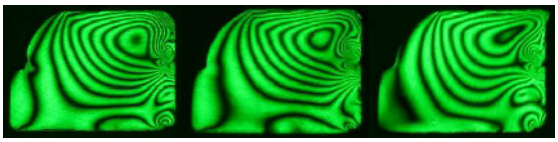

(d) 2.94 MPa (e) 3.92 MPa (f) 4.9 MPa

Fig. 4. Variation of isochromatic fringe patterns of a stress-frozen D-ring made from high temperature epoxy with internal pressure (H1/H2 = 1, r = 0.33 mm).

mm.

The maximum stresses (fillet radii) were 0.446 MPa (0.1 mm), 0.386 MPa (0.2 mm), 0.323 MPa (0.3 mm), 0.269 MPa (0.33 mm), 0.269 MPa (0.35 mm) and 0.269 MPa (0.4 mm), which shows that the maximum stresses at point 1_r described in Fig. 2(a) decreased as the fillet radius increased. Increasing the fillet radius beyond 0.33 mm did not cause a further decrease in stress intensity as shown in Table 1. As a result, a D-ring having a fillet radius of 0.33 mm was fabricated and used in this study.

Fig. 4 shows the isochromatic fringe patterns obtained from stress frozen D-rings with rounded corners compressed to a 20% squeeze as the internal pressure was varied from 0 to 4.9 MPa. As the internal pressure applied to the D-ring increased, the semi-circular portion moved over the step on the right side towards the restraining surface of the front side of the groove (see Fig. 2(b)). During the motion of the semi-circular portion, the space ahead of the step on the front side slowly filled up, and at a pressure of 2.94 MPa, the space was wholly filled. However, the semi-circular portion did not join with the rectangular part when the space ahead of the step on the front side became filled.

At a pressure of 0 MPa, the isochromatic fringe patterns of the stepped rounded D-ring are seen to be almost symmetrical. Although the fringe order did not change significantly as the applied internal pressure increased from 0 to 4.9 MPa, the vertical isochromatic fringe lines curved and shifted toward the front side. This made the upper and front sides of the D-ring the relatively stressed regions. As a result, the stresses on the upper and front sides of the D-ring were analyzed carefully. Moreover, significant attention was given to stresses developing in rounded corners in order to compare the results

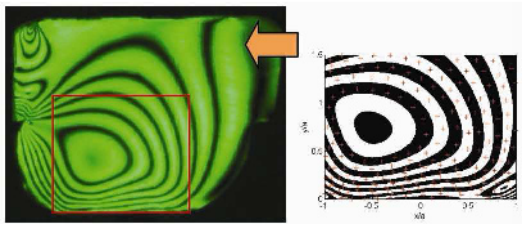

(a) Actual isochromatics (b) Graphic isochromatics

Fig. 5. Actual and graphic isochromatics of the upper side of a stepped rounded D-ring (squeeze rate = 20%, internal pressure = 0.98 MPa, a=1.72 mm, x = xu = -X, y = yu = -Y) from the photoelastic experimental hybrid method (the arrow indicates the direction of applied internal pressure).

with those from the stepped D-ring with unrounded corners. Extrusion of the stepped rounded D-ring occurred at an applied pressure of 4.9 MPa as shown in Fig. 4(f).

Although experiments involving six internal pressure cases of 0, 0.98, 1.96, 2.94, 3.92, and 4.9 MPa were carried out, only the results of internal stresses for three cases are reported in this paper. These are 0.98, 2.94, and 4.9 MPa.

In Fig. 5, the actual and graphic isochromatics of the upper region of the stepped rounded D-ring under a 20% squeeze rate and 0.98 MPa internal pressure are presented. The graphic isochromatics of the upper region of the stepped rounded D-ring under 20% squeeze rate and 0.98 MPa internal pressure and other regions hereafter, were obtained using stress components obtained from the photoelastic experimental hybrid method. The region highlighted by the rectangular box in the actual isochromatics represents the region with black and white bands from which experimental data were measured along the center lines. The cross marks "+" on the graphic isochromatics indicate the positions from which experimental data were measured. The similarity between the actual and graphic isochromatics shown in Fig. 5 is interesting. The cross marks "+" on the graphic isochromatics are located almost along the center lines of the isochromatic bands. This means that the photoelastic experimental hybrid method is valid for the stress analysis of a D-ring under a uniform squeeze rate and internal pressure. The x/a and y/a used in Fig. 5(b) and in the other figures hereafter denote the x and y distances, respectively normalized by one-half of the contact length, a, of the region selected for analysis.

Fig. 6 shows the contour lines depicting the internal stress components σ_X, σ_Y, and τ_{XY} normalized by internal pressure p_i for the upper side of the stepped rounded D-ring with a ratio of H_1/H_2 = 1 under 20% squeeze and 0.98 MPa internal pressure. The highest magnitudes of σ_X/p_i (σ_X) and σ_Y/p_i (σ_Y) were 3.6 (3.53 MPa) and 3.8 (3.72 MPa) respectively and those of τ_{XY}/p_i (τ_{XY}) were 0.12 (0.12 MPa). The magnitudes of shear stresses τ_{XY}/p_i were very low compared to σ_X/p_i and σ_Y/p_i.

Fig. 7 shows the contour lines showing the internal principal stresses σ_1, σ_2, τ_{12}, and Von Mises stresses σ_{VM},

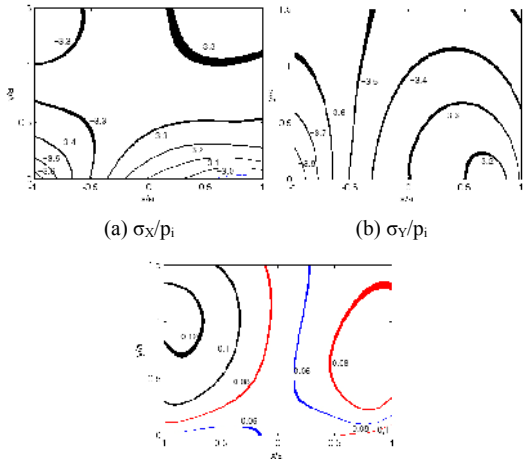

(a) σ_X/p_i (b) σ_Y/p_i

(c) τ_{XY}/p_i

Fig. 6. Normalized stress contours of the upper side of the stepped rounded D-ring with a ratio of H1/H2 = 1 (squeeze rate = 20%, internal pressure = 0.98 MPa, a = 1.72 mm, x = xu = -X, and y = yu = -Y).

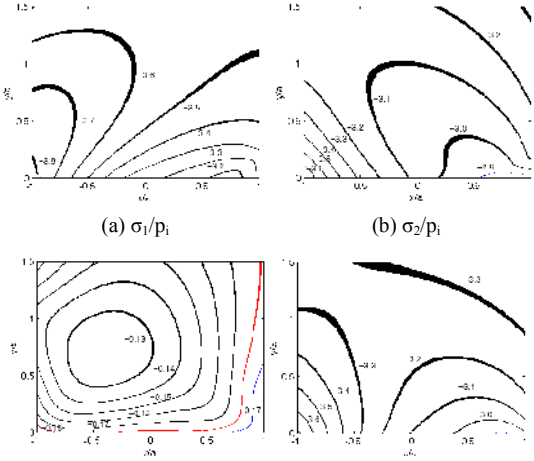

(a) σ_1/p_i (b) σ_2/p_i

(c) τ_{12}/p_i (d) σ_{VM}/p_i

Fig. 7. Normalized principal stress contours and von Mises stress contours of the upper side of the stepped rounded D-ring with a ratio of H_1/H_2=1 (squeeze rate = 20%, internal pressure = 0.98 MPa, a = 1.72 mm, x = xu = -X, y = yu = -Y).

normalized by internal pressure p_i for the upper side of the stepped rounded D-ring with a ratio of H_1/H_2 = 1 under 20% squeeze and 0.98 MPa internal pressure. The results indicate that the portion of the upper part closer to the extrusion gap was highly stressed. The highest magnitudes of σ_1/p_i (σ_1) and σ_2/p_i (σ_2) are 3.8 (3.72 MPa) and 3.6 (3.53 MPa), respectively, and those of τ_{12}/p_i (τ_{12}) and σ_{VM}/p_i (σ_{VM}) are 0.18 (0.18 MPa) and 3.6 (3.53 MPa), respectively. The contour lines of τ_{12}/p_i are similar to the actual isochromatics of the region highlighted by the rectangle. These results show that the photoelastic experimental hybrid method used in this research is valid for the stress analysis of structures. The magnitude of the principal shear stresses τ_{12}/p_i was significantly lower than those of σ_1/p_i, σ_2/p_i, and σ_{VM}/p_i.

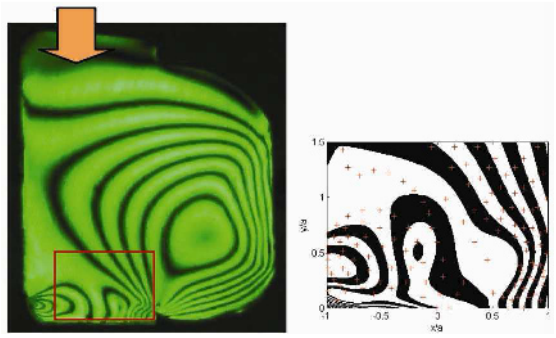

(a) Actual isochromatics (b) Graphic isochromatics

Fig. 8. Actual and graphic isochromatics of the front side of the stepped rounded D-ring (squeeze rate = 20%, internal pressure = 0.98 MPa, a=1.24 mm, x = xf = Y, and y = yf = -X) from photoelastic experimental hybrid method (arrow indicates direction of applied internal pressure).

The actual and graphic isochromatics of the front side of the D-ring under 20% squeeze and 0.98 MPa internal pressure are shown in Fig. 8. At a pressure of 0.98 MPa, only the rectangular portion of the stepped rounded D-ring was in contact with the restraining wall of the front side of the groove. Relatively high stresses were observed at point 1_r. The high stresses at point 1_r were due to the deformations resulting from the motion of the semi-circular portion over the step to fill the space ahead of it as internal pressure was increased. The groove profile at the corner between the lower and front walls seemingly had a considerable effect on the stresses at point 3_r because of the presence of high-order fringes at the point. A notable similarity between the actual and graphic isochromatics is seen in Fig. 8, and the cross marks "+" on the graphic isochromatics are located almost along the center lines of the isochromatic bands. This means that the photoelastic experimental hybrid method is valid for the stress analysis of the D-ring under a uniform squeeze rate and internal pressure.

Fig. 9 shows the stress contour lines depicting the internal principal stresses σ_1, σ_2, τ_{12}, and Von Mises stresses, σ_{VM} , normalized by internal pressure p_i, for the front side of the stepped rounded D-ring with a ratio of H_1/H_2 = 1 loaded at a 20% squeeze rate and 0.98 MPa internal pressure. The highest values of σ_1/p_i (σ_1) and σ_2/p_i (σ_2) are 2.4 (2.35 MPa) and 2.2 (2.16 MPa), respectively. The highest values of τ_{12}/p_i (τ_{12}), and σ_{VM}/p_i (σ_{VM}) are 0.12 (0.12 MPa) and 2.2 (2.16 MPa), respectively. The contour lines of τ_{12}/p_i are similar to the actual isochromatics of the region highlighted by the rectangle. It is therefore known through these results show that the photoelastic experimental hybrid method used in this research is valid in the stress analysis of structures.

Fig. 10 shows the actual and graphic isochromatics of the upper side of the stepped rounded D-ring with a ratio of H_1/H_2 = 1 for an applied internal pressure of 2.94 MPa and a squeeze rate of 20%. One-half of the contact length increased from 1.72 to 1.98 mm when the internal pressure was 0.98 MPa. Moreover, the fringes curved more toward the front side as the

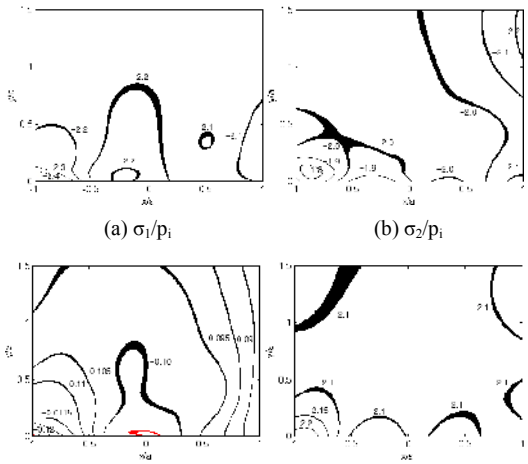

(a) σ_1/p_i (b) σ_2/p_i

(c) τ_{12}/p_i (d) σ_{VM}/p_i

Fig. 9. Normalized principal stress contours and von Mises stress contours of the front side of the stepped rounded D-ring with a ratio of H_1/H_2=1 (squeeze rate = 20%, internal pressure = 0.98 MPa, a = 1.24 mm, x = xf = Y, y = yf = -X).

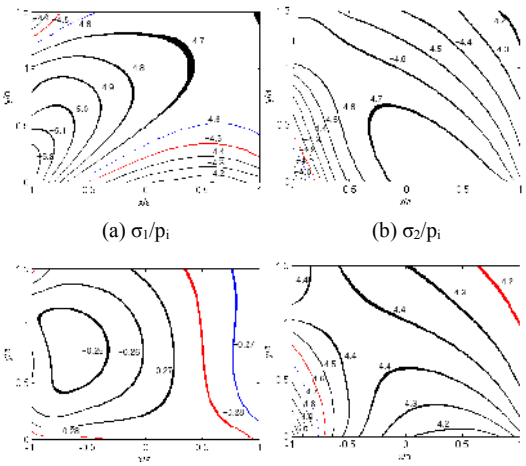

(a) σ_1/p_i (b) σ_2/p_i

(c) τ_{12}/p_i (d) σ_{VM}/p_i

Fig. 11. Normalized principal stress contours and von Mises stress contours of the upper side of the stepped rounded D-ring with a ratio of H_1/H_2=1 (squeeze rate = 20%, internal pressure = 2.94 MPa, a = 1.98 mm, x = xu = -X, and y = yu = -Y).

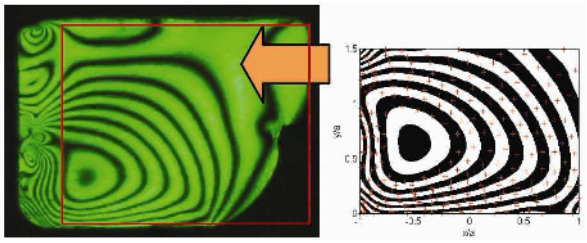

(a) Actual isochromatics (b) Graphic isochromatics

Fig. 10. Actual and graphic isochromatics of the upper side of a stepped rounded D-ring with a ratio of H_1/H_2=1 (squeeze rate = 20%, internal pressure = 2.94 MPa, a = 1.98 mm, x = xu = -X, and y = yu = -Y) from a photoelastic experimental hybrid method (the arrow indicates the direction of applied internal pressure).

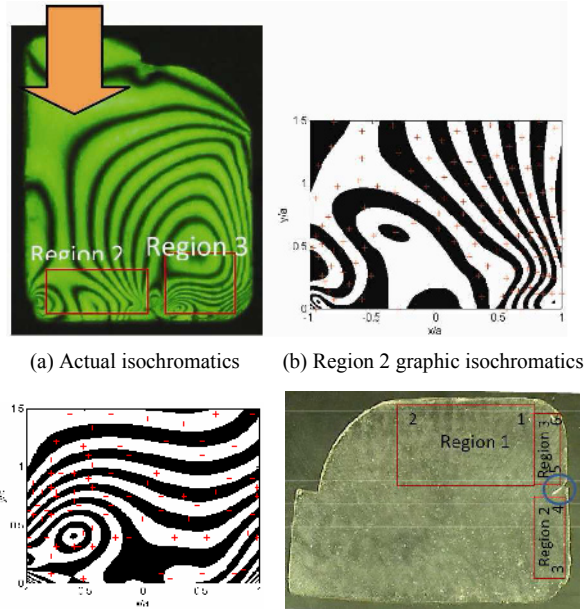

(a) Actual isochromatics (b) Region 2 graphic isochromatics

(c) Region 3 isochromatics (d) Video microscope image of (a)

Fig. 12. Actual (a); graphic (b~c) isochromatics and video microscope image (d) of the front side of D-ring (squeeze rate = 20%, internal pressure = 2.94 MPa, a = 1.52 mm (at region 2), a = 1.26 mm (at region 3), x = xf = Y, and y = yf = -X) from the photoelastic experimental hybrid method (arrow indicates direction of applied internal pressure).

pressure increased to 2.94 MPa. The actual isochromatics in the region highlighted by the rectangle are almost similar to the graphic isochromatics with the cross marks "+" on the graphic isochromatics located almost along the center lines of the isochromatic bands. Thus, the photoelastic experimental hybrid method is valid for the stress analysis of a D-ring under a uniform squeeze rate and internal pressure.

Fig. 11 shows the principal stress contour lines indicating the internal principal stresses σ_1, σ_2, τ_{12}, and Von Mises stresses σ_{VM}, normalized by internal pressure p_i, for the upper side of the stepped rounded D-ring with a ratio of H_1/H_2 = 1 loaded to 20% squeeze and 2.94 MPa internal pressure are shown in Fig. 11. The largest magnitudes of σ_1/p_i (σ_1) and σ_2/p_i (σ_2) are 5.2 (15.29 MPa) and 4.7 (13.82 MPa), respectively. The largest magnitudes of τ_{12}/p_i (τ_{12}) and σ_{VM}/p_i (σ_{VM}) are 0.28 (0.82 MPa) and 5.0 (14.7 MPa), respectively. The contour lines of τ_{12}/p_i are similar with the actual isochromatics of the region highlighted by a rectangle. Thus, these results show that the photoelastic experimental hybrid method used in this research is valid in the stress analysis of structures.

Fig. 12 shows the actual and graphic isochromatics of the front side of the stepped rounded D-ring with a ratio of H_1/H_2 = 1 loaded to a 20% squeeze and 2.94 MPa internal pressure. Application of an internal pressure of up to 2.94 MPa caused

the semi-circular portion of the stepped rounded D-ring with a ratio of $H_1/H_2 = 1$ to move over the step, fill the space ahead of it, and make contact with the restraining front wall of the groove. Due to the separation between the rectangular and semi-circular portions of the D-ring along 1_r-2_r (highlighted in Fig. 12(d)), the stresses over the entire front side could not be analyzed. Therefore, shown in Fig. 12, two regions (region 2 with position 3 and 4 as well as region 3 with position 5 and 6) of the front side were selected for analysis. A comparison between the actual isochromatics in the regions highlighted by the rectangle and the graphic isochromatics shows remarkable similarity. The cross marks "+" on the graphic isochromatics are located almost along the center lines of the isochromatic bands. This means that the photoelastic experimental hybrid method is valid for the stress analysis of a D-ring under uniform squeeze rate and internal pressure.

The stress contour lines depicting the internal stress components σ_X, σ_Y, and τ_{XY}, normalized by the internal pressure p_i, for the regions labeled 2 and 3 of the front side of the stepped rounded D-ring with a ratio of $H_1/H_2 = 1$ loaded to 20% squeeze and 2.94 MPa internal pressure are shown in Figs. 13 and 14, respectively. The highest magnitudes of σ_X/p_i (σ_X) and σ_Y/p_i (σ_Y) are 2.3 (6.76 MPa) and 2.45 (7.2 MPa), respectively, while those of τ_{XY}/p_i (τ_{XY}) are 0.05 (0.15 MPa) for region 2. The highest magnitudes of σ_X/p_i (σ_X) and σ_Y/p_i (σ_Y) are 2.5 (7.35 MPa) and 2.7 (7.94 MPa), respectively, and those of τ_{XY}/p_i (τ_{XY}) are 0.09 (0.26 MPa) for region 3. Since the values of stresses in region 2 are lower than those in region 3, the results of stresses analyzed from region 3 are reported hereafter. This is because this region included the relatively stressed areas of interest (the area in the vicinity of the step and that around the extrusion gap).

The principal stress contour lines depicting the internal principal stresses σ_1, σ_2, τ_{12}, and Von Mises stresses σ_{VM}, normalized by internal pressure p_i, for the regions labeled 2 and 3 of the front side of the stepped rounded D-ring with a ratio of $H_1/H_2 = 1$ loaded to 20% squeeze and 2.94 MPa internal pressure are shown in Figs. 15 and 16, respectively. The highest magnitudes of σ_1/p_i (σ_1) and σ_2/p_i (σ_2) are 2.4 (7.06 MPa) and 2.25 (6.62 MPa), respectively. For region 2, the highest magnitudes of τ_{12}/p_i (τ_{12}) and σ_{VM}/p_i (σ_{VM}) are 0.07 (0.21 MPa) and 2.35 (6.91 MPa), respectively. The highest magnitudes of σ_1/p_i (σ_1) and σ_2/p_i (σ_2) are 2.7 (7.94 MPa) and 2.42 (7.11 MPa), respectively, and those of τ_{12}/p_i (τ_{12}) and σ_{VM}/p_i (σ_{VM}) are 0.10 (0.29 MPa) and 2.5 (7.35 MPa), respectively, for region 3.

The contour lines of τ_{12}/p_i shown in Figs. 15 and 16 are similar to the actual isochromatics of the regions highlighted by the rectangle. Thus, these results show that the photoelastic experimental hybrid method used in this research is valid in the stress analysis of structures.

The actual and graphic isochromatics of the upper side of the stepped rounded D-ring with a ratio of $H_1/H_2 = 1$ loaded to a 20% squeeze and 4.9 MPa internal pressure are shown Fig. 17. An applied pressure of up to 4.9 MPa pushed the portion

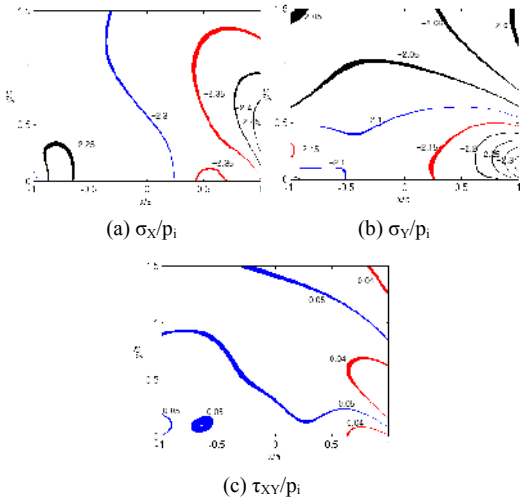

(a) σ_X/p_i (b) σ_Y/p_i

(c) τ_{XY}/p_i

Fig. 13. Normalized stress contours of the front side of the stepped rounded D-ring with a ratio of H_1/H_2=1 for region 2 (squeeze rate = 20%, internal pressure = 2.94 MPa, a = 1.52 mm, x = xf = Y, and y = yf = -X).

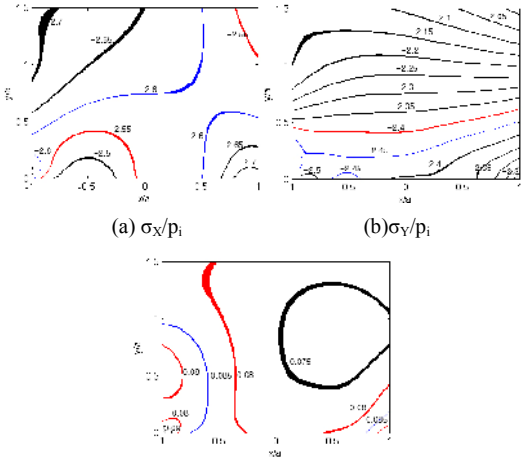

(a) σ_X/p_i (b)σ_Y/p_i

(c) τ_{XY}/p_i

Fig. 14. Normalized stress contours of the front side of the stepped rounded D-ring with a ratio of H_1/H_2=1 for region 3 (squeeze rate = 20%, internal pressure = 2.94 MPa, a = 1.26 mm, x = xf = Y, and y = yf = -X).

of the D-ring near the extrusion gap through the extrusion gap, causing extrusion. The pressure of 4.9 MPa also caused the isochromatic fringe lines to curve and concentrate around the extrusion gap. One-half of the contact length increased from 1.98 mm to 2.57 mm when internal pressure was 2.94 MPa. The actual isochromatics in the region highlighted by the rectangle are similar to the graphic isochromatics. The cross marks "+" on the graphic isochromatics are located almost along the center lines of the isochromatic bands. This means that the photoelastic experimental hybrid method is valid for stress analysis of a D-ring under a uniform squeeze rate and internal pressure.

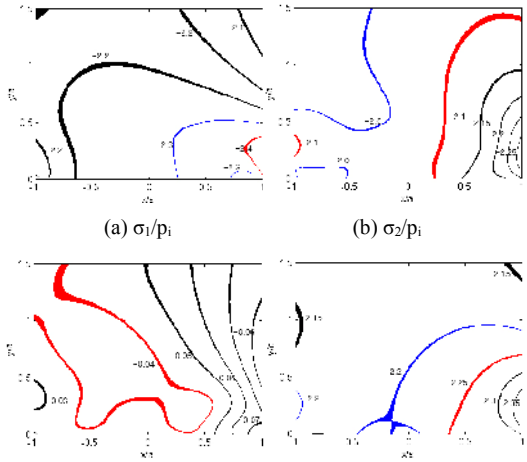

(a) σ_1/p_i (b) σ_2/p_i

(c) τ_{12}/p_i (d) σ_{VM}/p_i

Fig. 15. Normalized principal stress contours and von Mises stress contours of the front side of the stepped rounded D-ring with a ratio of H_1/H_2 = 1 for region 2 (squeeze rate = 20%, internal pressure = 2.94 MPa, a = 1.52 mm, x = xf = Y, and y = yf = -X).

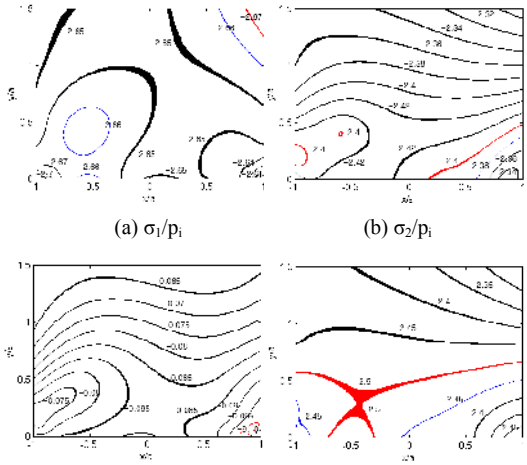

(a) σ_1/p_i (b) σ_2/p_i

(c) τ_{12}/p_i (d) σ_{VM}/p_i

Fig. 16. Normalized principal stress contours and von Mises stress contours of the front side of the stepped rounded D-ring with a ratio of H_1/H_2 = 1 for region 3 (squeeze rate = 20%, internal pressure = 2.94 MPa, a = 1.26 mm, x = xf = Y, and y = yf = -X).

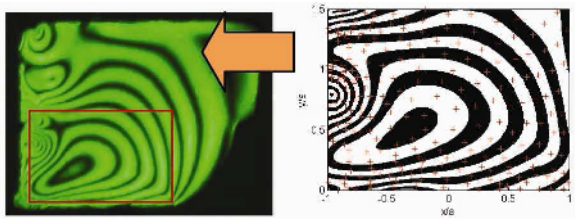

(a) Actual isochromatics. (b) Graphic isochromatics.

Fig. 17. Actual and graphic isochromatics of the upper side of the stepped rounded D-ring with a ratio of H_1/H_2=1 (squeeze rate = 20%, internal pressure = 4.9 MPa, a = 2.57 mm, x = xu = -X, and y = yu = -Y) from the photoelastic experimental hybrid method (the arrow indicates the direction of applied internal pressure).

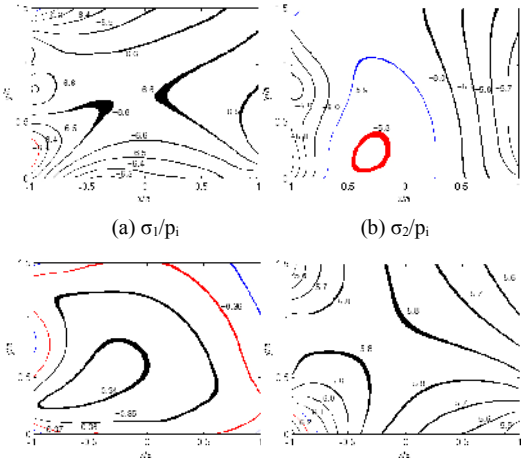

(a) σ_1/p_i (b) σ_2/p_i

(c) τ_{12}/p_i (d) σ_{VM}/p_i

Fig. 18. Normalized principal stress contours and von Mises stress contours of the upper side of the stepped rounded D-ring with a ratio of H_1/H_2=1 (squeeze rate = 20%, internal pressure = 4.9 MPa, a = 2.57 mm, x = xu = -X, and y = yu = -Y).

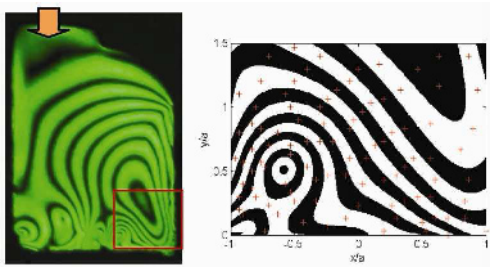

(a) Actual isochromatics (b) Graphic isochromatics

Fig. 19. Actual and graphic isochromatics of the front side of the stepped rounded D-ring with a ratio of H_1/H_2=1 (squeeze rate = 20%, internal pressure = 4.9 MPa, a = 1.35 mm, x = xf = Y, and y = yf = -X) from the photoelastic experimental hybrid method (the arrow indicates the direction of applied internal pressure).

Fig. 18 shows the stress contour lines describing the internal principal stresses σ_1, σ_2, τ_{12}, and Von Mises stresses, σ_{VM}, normalized by internal pressure p_i, for the upper side of the stepped rounded D-ring with a ratio of H_1/H_2 = 1 loaded to 20% squeeze and 4.9 MPa internal pressure. Relatively high stresses are observed in the vicinity of the extrusion gap. The highest magnitudes of σ_1/p_i (σ_1) and σ_2/p_i (σ_2) are 6.6 (32.34 MPa) and 6.0 (29.4 MPa), respectively, while those of τ_{12}/p_i (τ_{12}) and σ_{VM}/p_i (σ_{VM}) are 0.37 (1.81 MPa) and 6.2 (30.8 MPa), respectively. The contour lines of τ_{12}/p_i are similar to the actual isochromatics of the region highlighted by the rectangle.

Thus, these results show that the photoelastic experimental hybrid method used in this research is valid for the stress analysis of structures.

Fig. 19 shows the actual and graphic isochromatics of the front side of the stepped rounded D-ring with a ratio of H_1/H_2 = 1 loaded to a 20% squeeze and 4.9 MPa internal pressure. An applied pressure of up to 4.9MPa caused the semi-circular portion of the D-ring to move over the step and make contact

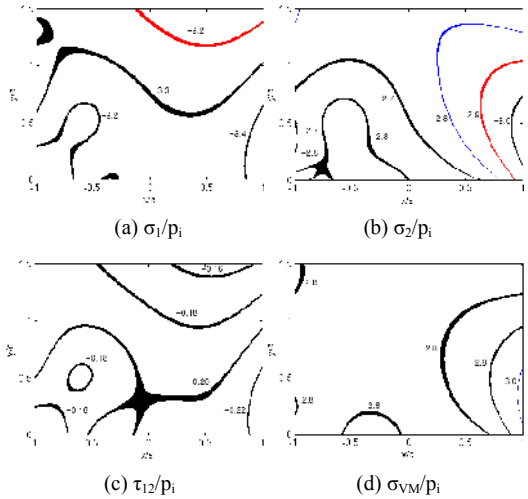

(a) σ_1/p_i (b) σ_2/p_i

(c) τ_{12}/p_i (d) σ_{VM}/p_i

Fig. 20. Normalized principal stress contours and von Mises stress contours of the front side of the stepped rounded D-ring with a ratio of H_1/H_2=1 (squeeze rate = 20%, internal pressure = 4.9 MPa, a = 1.35 mm, x = xf = Y, and y = yf = -X).

with the restraining front wall of the groove. The portion of the D-ring near the extrusion gap was pushed through the extrusion gap, causing extrusion to occur. One-half of the contact length in region 3 increased from 1.26 mm when the pressure was 2.94 MPa to 1.35 mm, and when the applied pressure was 4.9 MPa. The actual isochromatics in the region highlighted by the rectangle were almost similar to the graphic isochromatics with the cross marks "+" on the graphic isochromatics located almost along the center lines of the isochromatic bands. This means that the photoelastic experimental hybrid method is valid for stress analysis of a D-ring under a uniform squeeze rate and internal pressure.

Fig. 20 shows the stress contour lines describing the internal principal stresses σ_1, σ_2, τ_{12}, and von Mises stresses σ_{VM}, normalized by internal pressure p_i, for the front side of the stepped rounded D-ring with a ratio of H_1/H_2 = 1 loaded to 20% squeeze and 4.9 MPa internal pressure. The highest magnitudes of σ_1/p_i (σ_1) and σ_2/p_i (σ_2) are 3.4 (16.66 MPa) and 3.0 (14.7 MPa), respectively. The highest magnitudes of τ_{12}/p_i (τ_{12}) and σ_{VM}/p_i (σ_{VM}) are 0.22 (1.08 MPa) and 3.0 (14.7 MPa), respectively. The contour lines of τ_{12}/p_i are similar to the actual isochromatics of the region highlighted by the rectangle. Thus, these results show that the photoelastic experimental hybrid method used in this research is valid in the stress analysis of structures.

Upon extrusion at an internal pressure of 4.9 MPa, the highest magnitudes of principal stresses and von Mises stresses for both the upper and front sides of the stepped rounded D-ring were recorded near the extrusion gap (Figs. 18 and 20). The existence of high stresses near the extrusion gap at the time the extrusion begins suggests that failure of the stepped rounded D-ring is more likely to occur around the extrusion gap. In a previous study of the unrounded D-ring by the authors, it was found that extrusion occurred at an applied

Table 2. Effect of fillet radius on internal stress at a sharp corner of a stepped D-ring with a ratio of H_1/H_2 = 1.

Fillet radius, r = 0 mm		Fillet radius, r = 0.33 mm	
Applied internal pressure (MPa)	Internal stress σY/pi at end point(= x/a) -1	Internal stress σY/pi at end point(= x/a) -1	Percent reduction
0	-1.4567	-1.0956	25
0.98	-2.4137	-1.1537	11
1.96	-2.5762	-2.2805	11
2.94	-2.8145	-2.2397	20
3.92	-2.7817	-2.3801	14

Table 3. Highest maximum internal shear stresses normalized with respect to internal pressure for upper side of D-ring.

Internal pressure (MPa)	τ12/pi for stepped unrounded D-ring: H_1/H_2 = 1	τ12/pi for stepped rounded D-ring: H_1/H_2 = 1	Percent decrease
0	0.32	0.1	69
0.98	0.29	0.17	41
1.96	0.35	0.19	46
2.94	0.40	0.27	33
3.92	0.55	0.28	49

internal pressure of 3.92MPa. Nam et al. [16] reported that extrusion of the O-ring under a uniform squeeze rate and internal pressure occurred when the applied pressure was 1.96 MPa. In the present study, extrusion occurred after application of internal pressure of up to 4.9 MPa which is about 25% higher than the pressure at which extrusion initiated for a stepped unrounded D-ring. This means that the stepped rounded D-ring is better suited for a high pressure application and that the packing performance of the stepped rounded D-ring is better than the performance of either the stepped unrounded D-ring or the O-ring.

We determined whether the introduction of a fillet radius to the stepped unrounded D-ring with a ratio of H_1/H_2 = 1 played any significant role in decreasing the internal stresses at the end points as suggested by Miniatt et al. [17]. A comparison of the stresses at the end point(= x/a), -1 for the unrounded and rounded cases was performed and the results are summarized in Table 2. Supplying a fillet radius at the corners of the D-ring led to 25% reduction of the internal stresses at the corners of the stepped unrounded D-ring.

Table 3 shows the maximum internal shear stresses (τ_{12}/p_i) due to the stepped un-rounded and stepped rounded D-rings with a ratio of H_1/H_2 = 1. It is observed that the maximum internal shear stresses for the stepped rounded D-ring with a ratio of H_1/H_2 = 1 were lower than those of the stepped un-rounded D-ring with a ratio of H_1/H_2 = 1. The low magnitudes of the maximum shear stresses show that the stepped rounded D-ring is less vulnerable to shear failure compared to the stepped unrounded D-ring.

Comparison of internal stress components, principal stresses

and von Mises stresses between the stepped unrounded [18] and stepped rounded D-rings with $H_1/H_2 = 1$ showed that at the extrusion pressure, the stepped rounded D-ring had higher contact stresses than the stepped unrounded D-ring, further confirming its better packing ability.

The magnitudes of the shear stresses at the pressure at which extrusion occurred were considerably higher compared to the magnitudes before extrusion. This makes the maximum shear stress criterion on fracture more appropriate for D-rings.

5. Results and discussion

From our study of a stepped rounded D-ring with a ratio of $H_1/H_2 = 1$, the following conclusions are made:

(1) A fillet radius equal to one-half the distance between the vertical edge of the rectangular part of the D-ring and the intersection of the circular portion with the rectangular portion of 0.33 mm was found to be optimal for a stepped D-ring with a ratio of $H_1/H_2 = 1$.

(2) A fillet radius of 0.33 mm at the corners of the stepped D-ring with a ratio of $H_1/H_2 = 1$ led to a reduction of high internal stresses at the end points of the unrounded D-ring by about 25%.

(3) An internal pressure of 4.9 MPa is required to initiate extrusion in the stepped rounded D-ring with a ratio of $H_1/H_2 = 1$. An internal pressure of 3.92 MPa is required to commence extrusion in a stepped unrounded D-ring with a ratio of $H_1/H_2 = 1$.

(4) Comparison of internal stress components, principal stresses and von Mises stresses between stepped unrounded and stepped rounded D-rings with $H_1/H_2 = 1$ showed that at the extrusion pressure, the stepped rounded D-ring had higher internal stresses than the stepped unrounded D-ring and therefore better packing ability.

(5) The stress contour lines for each of the pressures investigated show high magnitudes of stress components, principal stresses, von Mises stresses at position 1 of region 1, position 3 of region 2, and position 6 of region 3. Comparing the magnitude of the highest stresses in contour lines of the stepped rounded D-ring with $H_1/H_2 = 1$ with those of the stepped unrounded D-ring with $H_1/H_2 = 1$, those in the stepped rounded D-ring with $H_1/H_2 = 1$ were lower for the same applied internal pressure.

(6) During the motion of the semi-circular portion, of the D-ring, space ahead of the step on the front side slowly filled. At a pressure of 2.94 MPa, the space was fully filled. However, the semi-circular portion does not join with the rectangular part when the space ahead of the step on the front side becomes filled.

References

[1] C.-Y. Lee, C.-S. Lin, R.-Q. Jian and C.-Y. Wen, Simulation and experimentation on the contact width and pressure distribution of lip seals, *Tribology International*, 39 (2006) 915-920.

[2] T. A. Stolarski and M. Tucker, Frictional performance of an O-ring type seal at the commencement of linear motion, *Tribology Letters 2* (1996) 405-416.

[3] Sealing Technology, Vol. 2007, Issue 8, 3-4, August 2007.

[4] H.-S. Lee, Y.-S. Lee, B.-S. Chun, S.-Y. Kim and J.-H. Baek, Contact stress analysis on the X-shape X-ring, *Materialwissenschaft und Werkstofftechnik,* 39 (2) (2008) 193-197.

[5] Parker Bulletin, Engineered Solutions, Issue 19, June 2010.

[6] A. F. George, A. Strozzi and J. I. Rich, Stress fields in a compressed unconstrained elastomeric O-ring seal and a comparison of computer predictions and experimental results, *Tribology International,* 20 (5) (1987) 237-247.

[7] A. Strozzi, Static stresses in an unpressurized, rounded, rectangular elastomeric seal, *Tribology Transactions*, 29 (4) (1986) 558-564.

[8] G. Medri and A. Strozzi, Mechanical analysis of elastomeric seals by numerical methods, *Ind. Eng. Chem. Prod. Res. Dev.*, 23 (1984) 596-600.

[9] C. Bignardi, A. Manuello Bertetto and L. Mazza, Photoelastic measurements and computation of stress field and contact pressure in a pneumatic lip seal, *Tribology International*, 32 (1999) 1-13.

[10] N. I. Muskhelishvili, *Some basic problems of the mathematical theory of elasticity*, 4th Edition Groningen, Netherlands: P. Noordhoff (1963).

[11] D. A. Hills, D. Nowell and A. Sackfield, *Mechanics of elastic contacts*, Butterworth-Heinemann, U.S.A. (1993).

[12] R. C. Sampson, A stress-optic law for photoelastic analysis of orthotropic composites, *Experimental Mechanics*, 10 (1970) 210-215.

[13] M. S. Bazaraa and C. M. Shetty, Nonlinear programming theory and algorithms, *John Wiley & Sons Inc*, (1979).

[14] Roy R. Craig, Jr., *Mechanics of materials*, 2nd Ed., John Wiley & Sons Inc (2000).

[15] J.-H. Nam, J.-S. Hawong, S.-L. Han and S.-H. Park, Contact stress of O-ring under uniform squeeze rate by photoelastic experimental hybrid method, *Journal of Mechanical Science and Technology*, 22 (2008) 2337-2349.

[16] J.-H. Nam, J.-S., D.-C. Shin and Bruno R. Mose, A study on the behaviors and stresses of O-ring under uniform squeeze rates and internal pressure by transparent type photoelastic experiment, *Journal of mechanical Science and Technology* (25) (2011) 2427-2438.

[17] E. C. Miniatt, A. M. Waas and W. J. Anderson, An experimental study of stress singularities at a sharp corner in a contact problem, *Experimental Mechanics*, (1990) 281-285.

[18] Bruno R. Mose, J.-S. Hawong, Bernard O. Alunda, H. S. Lim and J. H. Nam, Evaluating the stresses of a stepped unrounded D-ring under uniform squeeze rate and internal pressure by photoelastic experimental hybrid method, *Journal of Mechanical Science and Technology*, 26 (8) (2012) 2603-2616.

Jeong-hwan Nam received the B.S. degree in mechanical engineering in 1986 and the M.S. degree in 1996, both from Yeungnam University in Korea. He received the Ph.D. degree from Saitama Institute of Technology in Japan in 2005. He is currently a Professor at the Department of Railroad Vehicle Engineering at Dongyang University, Yeongju City, Korea. Prof. Nam's research interests are the areas of mechanical design, stress analysis, and experimental mechanics for stress analysis.

Jai-Sug Hawong received a B.S. degree in Mechanical Engineering from Yeungnam University in 1974. Then he received his M.S. degree and Ph.D. degree from Yeungnam University in Korea in 1976 and from Kanto Gakuin University in Japan in 1990, respectively. Prof. Hawong is currently a professor at the school of Mechanical Engineering at Yeungnam University, in Gyeongsan city, Korea. He served as President of Korean Society of Mechanical Engineering. Prof. Hawong's research interests include static and dynamic fracture mechanics, stress analysis, experimental mechanics for stress analysis and composite material, etc.